PROXIMITY OPERATIONS OF ON-ORBIT SERVICING SPACECRAFT USING AN ECCENTRICITY/INCLINATION VECTOR SEPARATION

J. Spurmann (1), S. D'Amico (2)
(1) DLR, German Space Operations Center, 82230 Wessling, joern.spurmann@dlr.de
(2) DLR, German Space Operations Center, 82230 Wessling, simone.damico@dlr.de

Abstract: *This paper investigates a proximity operations concept able to realize the demanding requirements for on-orbit servicing spacecraft, while providing an efficient collision avoidance strategy and reduced propellant consumption. In contrast to a traditional rendezvous approach where the evaluation of the collision risk is only based on considerations done in the orbital plane, here a relative eccentricity/inclination vector separation concept is proposed which promises improved flexibility, robustness and reduced inter-spacecraft separations at a minimal collision risk. In this paper the novel proximity operations concept, originally developed for geostationary satellites and already used to operate low Earth orbit formations, is adopted to support far and mid range operations of on-orbit servicing non-cooperative vehicles. After addressing the effects of the relevant differential perturbations, suitable nominal relative motion geometries are derived based on a real-world navigation accuracy analysis. Radar tracking data and GPS navigation solutions for the client and servicer satellites respectively are used to trade minimum safety separations and characteristics of the rendezvous entry gate. Finally a fuel-efficient formation keeping and reconfiguration strategy is designed based on analytical solutions of the proposed linear motion model.*

Keywords: *Eccentricity/Inclination Vector Separation, Autonomous Formation Control, Formation Flying, On-Orbit Servicing, Relative Navigation.*

1 Introduction

The capability to autonomously rendezvous and dock two spacecraft would provide benefits to multiple mission scenarios. The correction of launch failures is one relevant example. Usually, upon a malfunction of the upper stage of the launcher the spacecraft does not achieve its desired altitude or inclination. Such an injection error can in the most cases not be corrected by the spacecraft onboard propulsion system and the mission is lost or at least unable to achieve its primary objectives. In case an on-orbit servicing spacecraft is already in orbit within a fleet management program for example the injection error could be corrected and the overall success rate of space missions could be increased. Another applicable area for autonomous rendezvous and docking is the removal of space debris. Even if within the next 20 years no further launches of spacecraft would be performed a cascade of collisions starts enhancing the number of collision fragments and thereby the overall number of space debris particles [1]. In this context any activity preventing satellites from becoming uncontrolled debris would improve the situation. Exemplary it could be thought of repair or refueling activities close to the spacecraft end of life. Lifetime of satellites could be extended by taking over the attitude and orbit control functionalities in a docked configuration. In such an achieved combined configuration a re-entry of the coupled spacecraft could be performed as well. Accordingly, also the capability to remove space debris in general would be enabled.

As a result of the aforementioned mission applications the goal must be to perform rendezvous and docking with non-cooperative spacecraft and a proper de-orbiting for debris removal. For this purpose after launch and phasing a tailored formation flying configuration has to be established before going into the two dimensional approach for proximity operations. The concept of eccentricity/inclination vector separation [2] is the most suitable to achieve this objective, since it

provides a passively safe formation flying configuration and a straightforward capability for formation keeping and reconfiguration. Previous research in this field has already demonstrated the potential of this method for the GRACE [3] or the TerraSAR-X/TanDEM-X mission [4]. Further, the technology demonstration mission PRISMA has already demonstrated autonomous formation control based on relative eccentricity/inclination vectors in low Earth orbit [5].

However, the aforementioned formation flying missions rely on cooperative spacecraft. GPS navigation solutions and raw data are available on-board for real-time navigation and control tasks as well as on-ground for precise post-facto reconstruction of the relative motion. The real challenge with non-cooperative spacecraft in the frame of an on-orbit servicing mission is represented by the availability of absolute navigation data only. The relative motion can only be reconstructed on-ground based on measurement data types of absolute nature. As a consequence effects given by common error cancellation cannot be exploited like typically done in formation flying satellites embarking hardware of same build and type. To this end different data types are analyzed in this paper obtained from satellites mission flying in low Earth orbit. Among the data types are the GPS navigation solution, radar tracking data provided by Fraunhofer institute for high frequency physics and radar techniques (FHR, former FGAN) [6] and angle tracking data. From the performed analysis the most promising candidates will be used for a relative navigation accuracy analysis representative for an on-orbit servicing mission.

The presented relative navigation accuracy analysis drives the selection of the dimensions of the formation flying geometry. For this purpose the eccentricity/inclination vector separation method is introduced. Its main advantage is that radial and along-track motion are no longer considered alone, but instead a complete 3D motion with a separation in the radial/cross-track plane. The larger uncertainties in the along-track component resulting from navigation, atmospheric density uncertainty and maneuver execution errors can thus be avoided. Within the present work the parameterization of the relative motion in terms of relative eccentricity/inclination vectors is used for the first time to transfer the servicer to the rendezvous entry gate from which the two dimensional approach is initiated. With respect to this transfer a formation reconfiguration strategy will be derived with respect to minimum collision risk, minimum fuel consumption and the possibility to allow for frequent autonomous reconfigurations of the formation. An additional constraint regarded within the selection of the formation geometry is the visibility constraint for relative navigation sensors, which will be used for the close range approach during an on-orbit servicing mission. Finally, an effective and fuel efficient way for formation keeping at further distances is derived based on the e/i-vector separation.

2 Relative Motion

The proposed formation flying concept is based on the generalization of the eccentricity/inclination vector separation method. For the description of this concept first the parameterization of the relative motion will be described. It will build up from the unperturbed, perturbed and controlled motion description.

2.1 Unperturbed Motion

For convenience the client spacecraft is taken as a reference for the formation. In this context the servicing spacecraft will orbit around the client and its motion mapped in the relative coordinate frame. The absolute and relative orbit parameterizations in the Earth-Centered-Inertial (ECI) frame are given by the following equations [2].

$$\boldsymbol{\alpha} = \begin{Bmatrix} a \\ u \\ e_x \\ e_y \\ i \\ \Omega \end{Bmatrix} = \begin{Bmatrix} a \\ \omega + M \\ e\cos\omega \\ e\sin\omega \\ i \\ \Omega \end{Bmatrix} \quad \text{and} \quad \delta\boldsymbol{\alpha} = \begin{Bmatrix} \delta a \\ \delta\lambda \\ \delta e_x \\ \delta e_y \\ \delta i_x \\ \delta i_y \end{Bmatrix} = \begin{Bmatrix} (a_S - a)/a \\ (u_S - u) + (\Omega_S - \Omega)\cos i \\ e_{x_S} - e_x \\ e_{y_S} - e_y \\ i_S - i \\ (\Omega_S - \Omega)\sin i \end{Bmatrix} \tag{1}$$

The first half of the equation gives a parameterization in Keplerian elements. This is modified by adopting the eccentricity vector $\boldsymbol{e} = (e_x, e_y)^T$ and the mean argument of latitude u. The second half of equation (1) gives the parameterization of the relative motion in a set of relative orbital elements (ROE) derived from a non-linear combination of the absolute parameterization. The subscript S is introduced denoting quantities of the servicing spacecraft. The ROE set consists of a normalized semi-major axis difference δa and the relative mean longitude between the two spacecraft $\delta\lambda$. Additionally, the relative eccentricity and inclination vectors are introduced for which the following Cartesian and polar notations are applied [2].

$$\delta\mathbf{e} = \begin{Bmatrix} \delta e_x \\ \delta e_y \end{Bmatrix} = \delta e \begin{Bmatrix} \cos\varphi \\ \sin\varphi \end{Bmatrix} \quad \text{and} \quad \delta\mathbf{i} = \begin{Bmatrix} \delta i_x \\ \delta i_y \end{Bmatrix} = \delta i \begin{Bmatrix} \cos\vartheta \\ \sin\vartheta \end{Bmatrix} \tag{2}$$

The phases of the relative e/i-vectors are termed relative perigee φ and relative ascending node ϑ because they characterize the geometry of the relative orbit as seen by the Client spacecraft.

The relative motion is described in the RTN orbital frame centered on the Client spacecraft. The coordinate frame is defined by the unit vector in radial direction (positive outwards, R), the unit vector in along-track direction of the satellite motion (positive in flight direction, T) and the unit vector normal to the orbital plane in direction to the positive angular momentum vector (cross-track, N). The orbital motion within this frame can be linearized for near circular orbits and small separations compared to the orbit radius by the Hill-Clohessy-Wiltshire (HCW) equations. Those can be expressed in relative orbital elements with the mean argument of latitude as independent variable [2].

$$\begin{Bmatrix} \delta r_R / a \\ \delta r_T / a \\ \delta r_N / a \\ \delta v_R / v \\ \delta v_T / v \\ \delta v_N / v \end{Bmatrix} = \begin{Bmatrix} \delta a & -\delta e\cos(u-\varphi) \\ \delta\lambda - \frac{3}{2}\delta a(u-u_0) & +2\delta e\sin(u-\varphi) \\ & +\delta i\sin(u-\vartheta) \\ & +\delta e\sin(u-\varphi) \\ -\frac{3}{2}\delta a & +2\delta e\cos(u-\varphi) \\ & +\delta i\cos(u-\vartheta) \end{Bmatrix} \tag{3}$$

According to Eq. (3) the general bounded relative motion with zero differential semi-major axis is a tilted ellipse (Figure 1). Its dimension is defined by the relative eccentricity vector norm in the R-T plane and by the relative inclination vector norm in cross-track direction. The mean along-track separation between the two spacecraft is defined by $\delta\lambda$

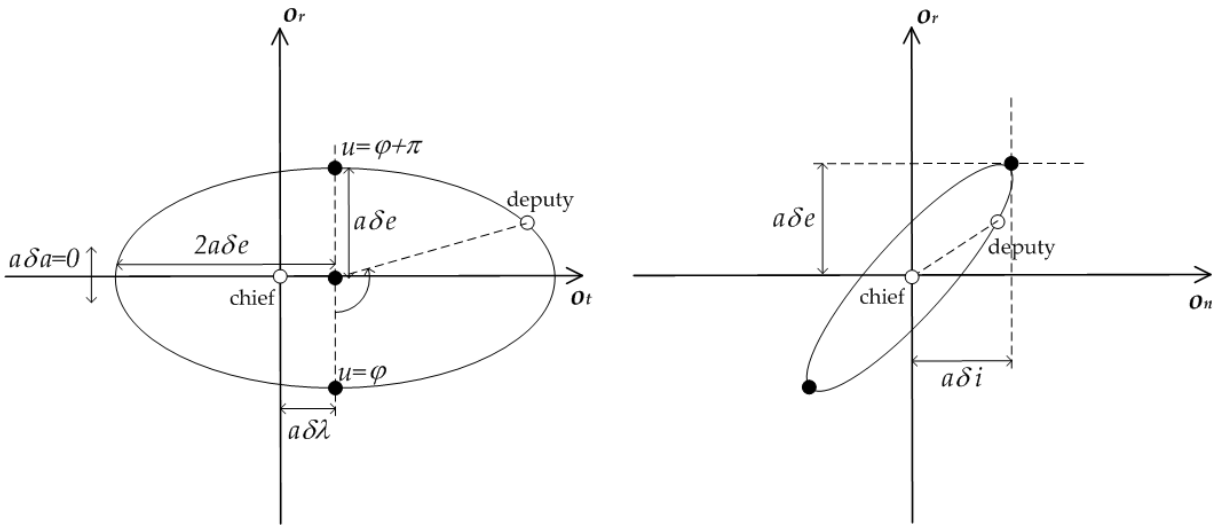

Figure 1. Projections of bounded relative motion in the along-track/radial (left) and cross-track/radial (right) directions for arbitrary relative orbital elements. Here Chief stands for Client spacecraft and Deputy for Servicer spacecraft.

2.2 Perturbed Motion

The natural motion from Eq. 3 can be extended by perturbations arising from Earth's oblateness effects J_2 and differential drag. Accordingly, a more efficient formation keeping strategy can be defined. The two perturbation terms, varying with time, are incorporated by summing them with a constant keplerian term.

$$\delta\boldsymbol{\alpha}(u) = \delta\boldsymbol{\alpha}(u_0) + \delta\delta\boldsymbol{\alpha}_{J_2}(u) + \delta\delta\boldsymbol{\alpha}_D(u) \tag{4}$$

The analytical treatment of the Earth's oblateness effects is based on the theory developed by Brouwer and Lyddane [6][8]. If only first-order terms in J_2 and e are considered in the series expansion the ROE can be expressed as a function of the mean argument of latitude u [2] (first term in Eq. 5).

For the atmospheric drag the main force is predominantly anti-parallel to the velocity of the spacecraft. As a result the differential drag has a linear impact on the relative semi-major axis and a quadratic impact on the relative mean argument of latitude (second term in Eq. 5).

$$\delta\boldsymbol{\alpha}(u) = \begin{Bmatrix} \delta a \\ \delta\lambda - \frac{21}{2}\gamma\sin(2i)\delta i_x(u-u_0) \\ \delta e\cos(\varphi+\varphi'(u-u_0)) \\ \delta e\sin(\varphi+\varphi'(u-u_0)) \\ \delta i_x \\ \delta i_y + 3\gamma\sin^2(i)\delta i_x(u-u_0) \end{Bmatrix} + \begin{Bmatrix} -\Delta B\rho a(u-u_0) \\ +\frac{3}{4}\Delta B\rho a(u-u_0)^2 \\ 0 \\ 0 \\ 0 \\ 0 \end{Bmatrix} \tag{5}$$

For the remaining coefficients in Eq. 5 ΔB is the difference between the spacecraft ballistic coefficients ($B = C_D A/m$), C_D the aerodynamic drag coefficient, A the cross-section area, m the satellite mass, ρ the atmospheric density and

$$\gamma = \frac{J_2}{2}\left(\frac{R_E}{a}\right)^2 \qquad \text{and} \qquad \varphi' = \frac{d\varphi}{du} = \frac{3}{2}\gamma\left(5\cos^2 i - 1\right). \tag{6}$$

Eq. (4) needs only to be substituted in Eq. (3) to obtain a first order solution of the equations of motion in the presence of J_2 and differential drag effects.

2.3 Controlled Motion

For inclusion of maneuvers into the relative motion model another term can be added to Eq. 4.

$$\delta\boldsymbol{\alpha}(u) = \delta\boldsymbol{\alpha}(u_0) + \delta\delta\boldsymbol{\alpha}_{J_2}(u) + \delta\delta\boldsymbol{\alpha}_D(u) + \delta\delta\boldsymbol{\alpha}_v(u) \tag{7}$$

More specific, this term results by inversion of the linear relative motion model. Thus the consequent change of ROE from an impulsive maneuver is given by

$$\delta\delta\boldsymbol{\alpha}_v = \begin{Bmatrix} \delta\delta a \\ \delta\delta\lambda \\ \delta\delta e_x \\ \delta\delta e_y \\ \delta\delta i_x \\ \delta\delta i_y \end{Bmatrix} = \frac{1}{na}\begin{Bmatrix} +2\delta v_T \\ -2\delta v_R - 3(u-u_M)\delta v_T \\ +\delta v_R \sin u_M + 2\delta v_T \cos u_M \\ -\delta v_R \cos u_M + 2\delta v_T \sin u_M \\ +\delta v_N \cos u_M \\ +\delta v_N \sin u_M \end{Bmatrix}. \tag{8}$$

Eq. (8) shows the result of an applied thrust at mean argument of latitude u_m. In addition a net change of mean longitude within the time interval between the maneuver execution and the epoch of the relative orbital elements results.

Two fundamental aspects should be noted from Eq. (8) for a proper choice of the formation keeping and reconfiguration strategy. First of all the in-plane and out-of-plane relative motions are decoupled. Maneuvers in cross-track direction only affect the relative inclination vector, while the other maneuver types only vary the in-plane component. Secondly, radial maneuvers are two times more expensive than along-track pulses for changes of the relative eccentricity vector and do not affect the semi-major axis.

3 Passive Safety and Stability

The relative e/i-vector separation concept is derived from the aforementioned linearized relative motion model and can be used to design proximity operations geometries characterized by minimum collision risk (passive safety) and minimum correction effort (passive stability). The concept of e/i-vector separation has originally been developed for the safe collocation of geostationary satellites [9], but can equally be applied to proximity operations for formation flight in LEO (GRACE, TerraSAR-X/TanDEM-X, PRISMA) [2]. It is based on the consideration that the uncertainty in predicting the along-track separation of two spacecraft is generally much higher than for the radial and cross-track component. Due to the coupling between semi-major axis and orbital period, small uncertainties in the initial position and velocity result in a corresponding drift error and thus a secularly growing along-track error. Predictions of the relative motion over extended periods of time are therefore particularly sensitive to both orbit determination errors and maneuver execution errors. To avoid a collision hazard in the presence of along-track position uncertainties, a proper separation of the two spacecraft in radial and cross-track direction is desirable. More specific the collision risk is defined by the minimum separation perpendicular to the flight direction (Eq. 9) for an arbitrary set of ROE [10].

$$\left(\frac{\delta r_{\min}}{a}\right)^2 \geq \frac{2(\delta\mathbf{e}\cdot\delta\mathbf{i})^2}{\left(\delta e^2+\delta i^2+|\delta\mathbf{e}+\delta\mathbf{i}|\cdot|\delta\mathbf{e}-\delta\mathbf{i}|\right)}+\delta a^2-2\delta a\delta e = \overset{\delta\mathbf{e}\,//\,\delta\mathbf{i}}{=} \min\{\delta e,\delta i\}^2+\delta a^2-2\delta a\delta e \tag{9}$$

For bounded relative motion ($\delta a = 0$), the minimum collision risk is provided by parallel or anti-parallel relative e/i-vectors ($\varphi = \vartheta$ or $\varphi = \vartheta+\pi$). For this configuration the formation is always separated in the NR plane in contrast to perpendicular relative e/i-vectors, for which radial and cross-track separation vanishes at the same time.

Concerning Eq. 9 another effect on formation reconfiguration shall be noticed. Using along-track maneuvers, the relative orbit ellipse is shifted in radial direction equal to the variation of the semi-major axis δa induced by the maneuver. In the case that $\delta a \geq 2\delta e$ the formation geometry remains safe, whereas for $\delta a < 2\delta e$ the minimum separation decreases. The latter situation is typical of formation keeping scenarios. This phenomenon makes along-track pulses inherently less safe than radial ones, but can be compensated by a suitably increased relative e/i-vector separation.

Concerning J_2 within the design of a passively safe formation the absolute inclination of the formation should ideally be identical to avoid a secular motion of the relative inclination vector (Eq. 5). Nevertheless, separation of the two orbital planes can be achieved by a small offset in the right ascensions of their ascending nodes. The resulting relative inclination vector has a phase angle $\vartheta = \pm\pi/2$, and the same (or opposite phase) must be selected for the relative eccentricity vector to obtain a passively safe formation. Adding the necessary condition for bounded relative motion of the servicer with respect to the client one obtains the following convenient nominal configuration

$$a\delta\boldsymbol{\alpha}_{\text{nom}} = \begin{Bmatrix} 0 \\ a\delta\lambda_{\text{nom}} \\ 0 \\ \pm a\delta e_{\text{nom}} \\ 0 \\ \pm a\delta i_{\text{nom}} \end{Bmatrix} \tag{10}$$

which provides passive stability and passive safety to the formation. The actual choice of the nominal relative orbital elements has to be done such that

$$\min\{a\delta e_{\text{nom}}, a\delta i_{\text{nom}}\} \geq d \tag{11}$$

where d represents a safety threshold for the minimum separation perpendicular to the flight direction. For the definition of d the following main contributions have to be considered:

1. Relative eccentricity and inclination vectors can only be controlled down to a certain accuracy depending on the applied control scheme, the navigation errors and the maneuver execution errors.
2. Formation reconfigurations in along-track direction, or rendezvous maneuvers require the execution of along-track pulses which affect the relative semi-major axis.
3. The minimum allowed separation between the center of mass shall take into account the physical dimensions of the spacecraft.
4. A heuristic margin of 50% is typically applied for safety reasons.

The overall contribution budget for the computation of d can be easily estimated based on the following considerations. The physical dimensions of the two spacecraft should not extend 10m on

the relative scale. Further, the maximum semi-major axis variation is proportional to the applied maneuver and thus strictly dependent on operational constraints like rendezvous time. The contribution will be derived within the design of the formation keeping and reconfiguration maneuvers later on. Finally, the expected orbit control accuracy will be derived based on the navigation accuracy analysis described in the next section.

4 Absolute Navigation Accuracy

The goal of this section is to derive the accuracy of a post-fact absolute orbit determination based on measurement data types which may be available in an on-orbit servicing scenario. Here GPS navigation solutions, radar tracking and angle tracking data are considered and their performance compared for a typical mission scenario. The analysis is performed on flight data of the currently operated missions at the German Space Operations Center (GSOC) CHAMP, GRACE and TerraSAR-X. The analysis was repeated for multiple missions to yield a first indication of an altitude profile. At the time of analysis CHAMP was flying at 325 km altitude, GRACE at 485 km and TerraSAR-X at 525 km. Since dual-frequency GPS raw data from receivers of geodetic quality are available for all missions a precise orbit determination (POD) with accuracy at cm level can be used as reference. The navigation accuracy can be derived from the comparison of the ephemeris resulting during analysis to the POD.

For the different tracking data types an orbit determination is performed over 24 hours, as in a typical flight operations scenario. An orbit prediction arc is appended to the end of the orbit determination arc. The ephemeris from propagation will be compared with the POD after 90minutes, 12 hours and 24 hours. Hence, an indication of the error development can be retrieved.

The position and velocity errors of the comparison are given below (Table 1). The errors are given as the root mean square (RMS) in each component of the RTN frame for the mentioned missions and the corresponding tracking data type.

Orbit determination errors based on angle tracking data are roughly one order of magnitude worse compared to GPS or radar tracking already after orbit determination. Accordingly, this measurement type has not been considered any further during the analysis. Furthermore, this data type would require an active logging of the spacecraft onboard transponder by the ground station. Hence, the applicability for on-orbit servicing missions as defined above is rather low since it requires a remaining functionality of the client spacecraft.

Orbit determination errors based on GPS and radar tracking show errors in the same order of magnitude for position and velocity. Radar tracking results are slightly worse compared to GPS especially at higher altitudes. In general the overall error trend decreases with higher altitudes.

As expected the largest contribution to the error budget is given by the along-track component. In fact the navigation error in along-track direction after 24 hour propagation is one (TX1) or two (CMP) orders of magnitude higher than the orbit determination accuracy depending on the orbit altitude. For the radial and cross-track component the navigation error stays within the same order of magnitude for both considered tracking data types.

The results from this section show that orbit determination can be performed based on radar tracking data for the client and on GPS navigation solution for the servicer, while leading to similar navigation errors. Hence, an adequate choice for an on-orbit servicing representative scenario can be made. Furthermore, the higher accuracy in radial and cross-track component over along-track justifies once more the design choice based on the e/i-vector separation concept.

Table 1. Absolute Navigation Errors

Position		RMS [m]					
		GPS			RADAR		Angle
		CMP	GRA	TX1	CMP	TX1	TX1
Radial	OD Acc	4.6	2.4	2.2	8.4	8.0	154.3
	90 min	6.9	3.4	0.6	8.0	8.1	
	12 h	13.7	5.5	3.1	12.1	5.9	
	24 h	18.9	6.4	3.6	17.7	6.0	
Along-track	OD Acc	13.4	7.4	6.0	31.2	29.6	374.0
	90 min	97.7	11.9	4.2	74.8	40.3	
	12 h	474.3	27.6	18.6	434.5	69.9	
	24 h	1 230.9	39.5	60.6	1 168.2	137.4	
Cross-track	OD Acc	9.8	3.5	2.8	10.8	5.3	34.6
	90 min	19.5	5.8	3.4	21.8	7.3	
	12 h	16.2	6.7	2.5	18.4	6.6	
	24 h	14.4	6.3	3.0	16.4	6.1	
Velocity		RMS [mm/s]					
		GPS			RADAR		Angle
		CMP	GRA	TX1	CMP	TX1	TX1
Radial	OD Acc	12.9	7.0	6.2	31.4	25.9	
	90 min	111.4	11.8	4.4	85.7	42.7	
	12 h	543.2	29.1	19.7	498.0	77.6	
	24 h	1 412.6	42.3	67.2	1 340.9	152.8	
Along-track	OD Acc	5.3	2.6	2.6	9.5	8.5	
	90 min	5.9	3.9	0.7	7.4	8.8	
	12 h	10.4	6.1	0.3	8.0	6.3	
	24 h	12.2	7.2	3.8	10.7	6.3	
Cross-track	OD Acc	11.6	3.8	3.1	11.2	6.2	
	90 min	25.0	5.7	3.8	26.9	10.1	
	12 h	35.1	8.3	3.1	35.7	10.0	
	24 h	72.7	8.3	5.2	71.2	12.8	

What is still unknown is the degree of correlation and the level of common error cancellation that can be expected from the subtraction of orbit determination results in order to obtain the desired relative state. Such problem will be addressed in the next section. So far the propagation error trends from the absolute orbit determination analysis show a high similarity for GPS and radar tracking performance. Possibly even smaller navigation errors can be expected from the relative navigation which may lead to a further reduction of the safety threshold d for the selection of the nominal formation flying configuration.

5 Relative Navigation Accuracy

The relative navigation accuracy analysis makes use of the same flight data as used in the previous section. Similarly the orbit determination accuracy is evaluated by comparing results based on different tracking data with the available precise orbit determination products. Since flight data from radar tracking and GPS are not currently available from co-orbiting satellites, the relative navigation accuracy analysis is here performed as a sort of zero-baseline test. On-ground orbit determination and prediction are performed for the same spacecraft based on different data types.

orbit determination and propagation is performed for the same spacecraft based on different tracking data types. GPS navigation solutions are used to represent the servicer and radar tracking data represent the client. Since the same spacecraft is considered the same POD product is used for both and cancels out during subtraction of the obtained ephemeris. The relative navigation errors obtained from the ground-based orbit determination are listed in Table 2.

Table 2. Relative Navigation Errors

		Position		Velocity	
		RMS [m]		RMS [mm/s]	
		CMP	TX1	CMP	TX1
Radial	OD Acc	6.7	7.8	28.6	31.3
	90 min	6.8	7.7	26.5	46.9
	12 h	6.8	7.8	47.0	62.8
	24 h	6.8	7.8	74.1	89.6
Along-track	OD Acc	27.4	31.1	7.8	8.5
	90 min	26.2	43.9	7.8	8.3
	12 h	42.8	57.3	7.8	8.5
	24 h	65.8	81.4	7.8	8.5
Cross-track	OD Acc	2.2	4.2	3.2	6.0
	90 min	2.3	4.3	2.4	6.8
	12 h	2.3	4.5	2.5	7.5
	24 h	2.3	4.5	3.1	8.7

As shown in Table 2, relative radial and cross-track components are characterized by errors below 10 m (RMS). It is noted that the propagation error is comparable with the orbit determination error and basically does not increase over time. A further comparison with the absolute orbit determination accuracy figures (cf. Table 1) shows that the orbit prediction is characterized by a high level of common error cancellation, while the orbit determination errors are un-correlated. As expected the relative navigation errors in along-track direction are gradually increasing over time but with a magnitude which is 10 times smaller than the absolute errors.

However it has to be noted that for this analysis orbit determination and propagation have been performed for the same spacecraft. The actual relative navigation error may be affected by mismodelling of differential accelerations caused e.g. by differential drag, especially at low altitudes as in the case of CHAMP.

Table 3. Differential Eccentricity and Inclination

		RMS [m]			RMS [m]	
		CMP	TX1		CMP	TX1
OD Acc	$a\delta ex$	6.0	6.0	$a\delta ix$	2.8	3.1
90 min		5.7	5.7		2.8	3.1
12 h		5.6	5.6		2.8	3.2
24 h		5.4	5.4		2.8	3.2
OD Acc	$a\delta ey$	7.5	7.5	$a\delta iy$	1.4	5.1
90 min		7.8	7.8		1.6	5.3
12 h		7.8	7.8		1.7	5.4
24 h		8.0	8.0		1.8	5.5

As described in section 3, the design of nominal formation flying configurations is driven by the relative control tracking errors and in turn by the relative navigation errors. In view of the adopted

parameterization of the relative motion, the relative navigation errors are further expressed in terms of relative eccentricity and inclination vectors. Table 3 shows that the expected relative navigation errors from on-ground orbit determination based on GPS and radar tracking data are of the order of 10 m (RMS).

As a consequence it can be finally concluded from the results that the maximum navigation error in $a\delta e$ and $a\delta i$ is always smaller than 10 m for parallel or anti-parallel relative e-/i-vectors.

6 Guidance and Control

The relative navigation results presented in the previous section give us the possibility to select a trade-off formation flying configuration which is inherently safe and stable (cf. section 3). Once the initial and final desired formation geometries are assigned, a formation keeping and reconfiguration strategy can be designed which takes advantage of the relative orbital element parameterization.

6.1 Nominal Formation Geometry

The first objective to derive the nominal formation geometry is to finalize the discussion from section 3 on the definition of the safety threshold d. The different contributions are again shown in Eq. 12.

$$d = \left\lfloor \max\left\{ a\delta e_{\mathrm{NavAcc}}, a\delta i_{\mathrm{NavAcc}} \right\} \cdot F_{Ctrl} + a\delta\delta a_{\delta v_T} + D_{Phys} \right\rfloor \cdot F_{mrg} \tag{12}$$

The contributions arise as follows:

1. The maximum navigation error in $a\delta\boldsymbol{e}$ and $a\delta\boldsymbol{i}$ is derived to be 10m.
2. An impulsive orbit control scheme is considered where the navigation accuracy can be considered as 10% of the controlled range ($F_{\mathrm{Ctrl}} = 10$).
3. Given a desired maximum along-track drift for rendezvous of 1.7 km/rev, the maximum necessary along-track impulse amounts to $\delta v_{\mathrm{T}} = 10$ cm/s. The resulting maximum semi-major axis variation amounts to $a\delta\delta a_{\delta v} = 185$ m.
4. The minimum allowed center of mass separation is taken as $D_{Phys} = 10$ m to account for the spacecraft physical dimensions.
5. A heuristic margin of 50% is typically applied for safety reasons ($F_{mrg} = 1.5$).

According to Eq. 12, the minimum separation safety threshold amounts to 450 m.

From the derived safety threshold the strategy to reconfigure the formation from an initial nominal formation configuration to a so called rendezvous entry point can now be developed employing the relative e/i-vector separation concept. The initial formation configuration is identified by Eq. (10). The rendezvous entry point is an arbitrary relative position $E = (E_{\mathrm{R}}, E_{\mathrm{T}}, E_{\mathrm{N}})^{\mathrm{T}}$ defined in the RTN orbital frame. From the initial conditions it is always possible to define a bounded relative orbit through (anti-)parallel relative e/i-vectors which contains the rendezvous entry point (Figure 2). By construction, the final formation geometry will provide the possibility to revisit the rendezvous entry point at each orbital revolution (Figure 2).

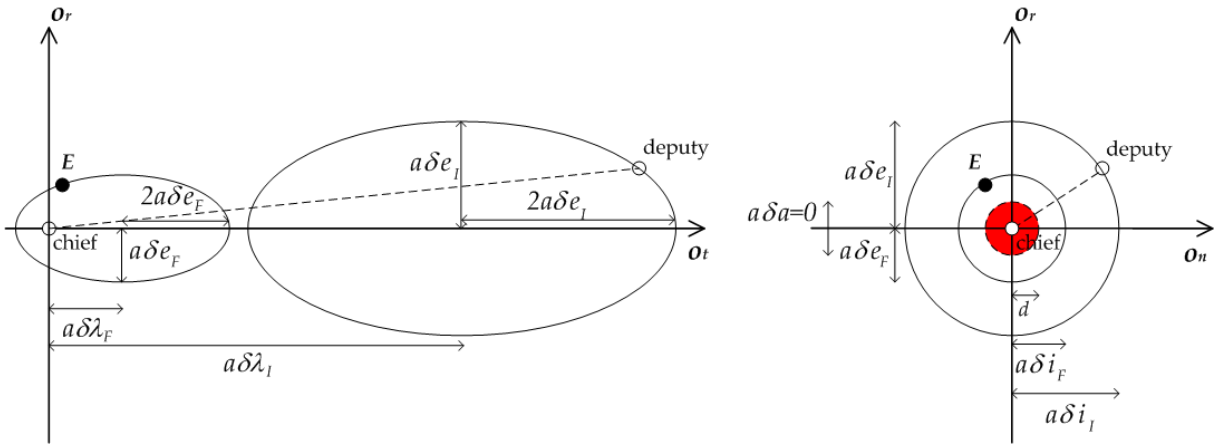

Figure 2. Relative orbit geometries for the formation reconfiguration problem. The initial relative orbital elements are identified by the subscript *I*, the final relative orbital elements are identified by the subscript *F*, the rendezvous entry point is identified by *E*, while the red circle of radius *d* represents the collision avoidance zone.

The initial formation flying configuration can be chosen according to Eq. 10 as

$$\{a\delta\lambda_I, a\delta e_I, a\delta i_I\}^T = \{2d/0.577, 2d, 2d\}^T = \{1560, 900, 900\}^T \text{ m}. \tag{13}$$

The selection of the nominal mean along-track separation is mainly driven by visibility constraints given by the relative navigation sensors during various operational scenarios. In the sequel the following choice has been made

$$\max\{a\delta e_{\text{nom}}, a\delta i_{\text{nom}}\}/a\delta\lambda_{\text{nom}} \geq \tan(30^o) = 0.577. \tag{14}$$

The final ROE set shall contain the rendezvous entry point within a three dimensional ellipse characterized by (anti-)parallel relative eccentricity and inclination vectors. For an arbitrary rendezvous entry point $E = (580,20,154)^T$ outside the collision avoidance zone the solution is simply given by

$$\{a\delta\lambda_F, a\delta e_F, a\delta i_F\}^T = \left\{E_T \pm 2\sqrt{a\delta e_F^2 - E_R^2}, \sqrt{E_N^2 + E_R^2}, a\delta e_F\right\}^T = \{327, 600, 600\}^T \text{ m} \tag{15}$$

Having defined three of the six parameters necessary to define a relative orbit by the equations above the missing parameters are the relative semi-major axis, which is set to zero to avoid diverging drifts, and the phases φ and ϑ which should guarantee the anti-parallelism of the relative e/i-vectors (i.e., $\varphi = -\vartheta = \pi/2$). In accordance with Eq. 10 the initial and final relative orbital elements for the representative scenario are given by

$$a\delta\boldsymbol{\alpha}_I = \begin{Bmatrix} 0 \\ a\delta\lambda_I \\ 0 \\ -a\delta e_I \\ 0 \\ a\delta i_I \end{Bmatrix} = \begin{Bmatrix} 0 \\ 1560 \\ 0 \\ -900 \\ 0 \\ 900 \end{Bmatrix} \text{m} \qquad a\delta\boldsymbol{\alpha}_F = \begin{Bmatrix} 0 \\ a\delta\lambda_F \\ 0 \\ -a\delta e_F \\ 0 \\ a\delta i_F \end{Bmatrix} = \begin{Bmatrix} 0 \\ 327 \\ 0 \\ -600 \\ 0 \\ 600 \end{Bmatrix} \text{m} \tag{16}$$

6.2 Formation Reconfiguration

The basic concept for the derived representative formation reconfiguration in case of an on-orbit servicing mission is illustrated in Figure 3. The intended transfer of the servicer to the rendezvous entry gate from which the two dimensional approach is initiated is shown in the left subplot by the corrections necessary to the relative e/i-vectors.

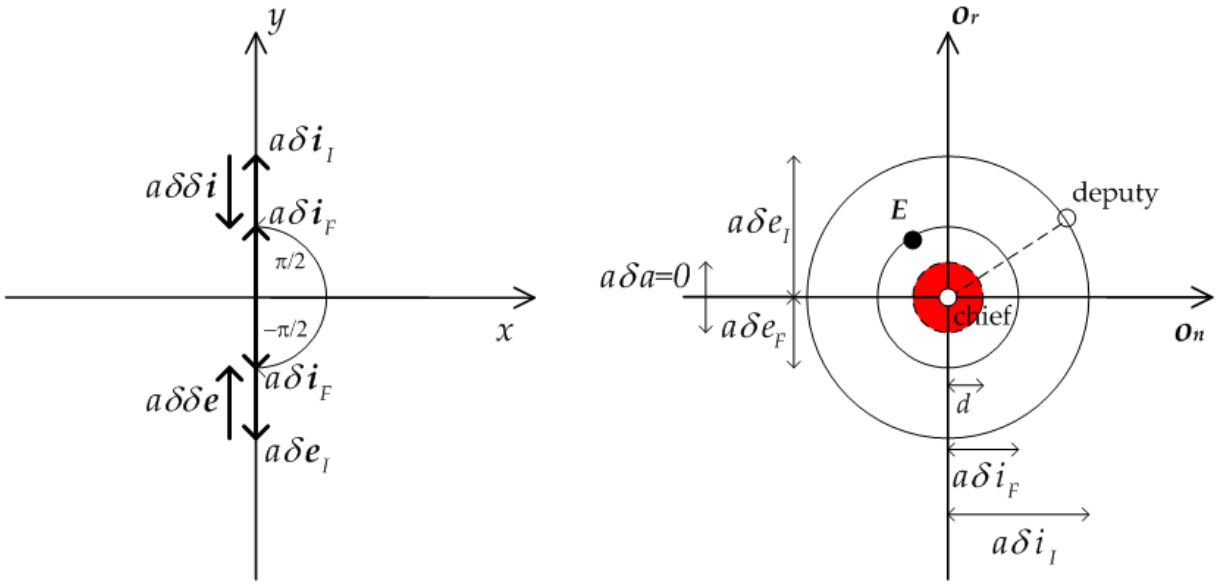

Figure 3. Anti-parallel relative eccentricity and inclination vectors for the formation reconfiguration (left) and corresponding relative motion in the plane perpendicular to the flight direction (right).

The corrections required for reconfiguration are given by

$$a\delta\boldsymbol{\alpha} = a\delta\boldsymbol{\alpha}_F - a\delta\boldsymbol{\alpha}_I = \begin{Bmatrix} 0 \\ a\delta\lambda_F - a\delta\lambda_I \\ 0 \\ -a\delta e_F + a\delta e_I \\ 0 \\ a\delta i_F - a\delta i_I \end{Bmatrix} = \begin{Bmatrix} 0 \\ a\delta\delta\lambda \\ 0 \\ a\delta\delta e_y \\ 0 \\ a\delta\delta i_y \end{Bmatrix} = \begin{Bmatrix} 0 \\ -1233 \\ 0 \\ 300 \\ 0 \\ -300 \end{Bmatrix} \text{m} . \tag{17}$$

In-plane and out-of-plane relative orbit control problems are decoupled. One cross-track maneuver is necessary and sufficient to control the relative inclination vector, while two in-plane maneuvers are necessary and sufficient to correct relative eccentricity vector and relative semi-major axis. The in-plane maneuvers may be implemented as radial, along-track or mixed radial/along-track pulses. In general the advantages of radial maneuvers reside in their larger size since resulting in smaller execution errors for small impulse bits and in the fact that radial maneuvers do not affect the semi-major axis. Such advantages can be exploited during on-orbiting servicing phases with small inter-spacecraft separations and higher control accuracy requirements. The advantages of along-track maneuvers lie in their smaller size (half of the radial maneuvers) and in the capability to change the semi-major axis for fuel-efficient rendezvous operation phases.

A design of the outlined transfer using one radial and one cross-track maneuver pair, while reducing the mean along-track separation at the same time results in the following ΔV maneuver plan.

$$\begin{cases} \delta v_{R1} = +na\|\delta\delta\mathbf{e}\|/2 - na\delta\delta\lambda/4 = 0.495\,\text{m/s} & u_{R1} = \text{atan}\left(\delta\delta e_y/\delta\delta e_x\right) + \pi/2 = \pi \\ \delta v_{R2} = -na\|\delta\delta\mathbf{e}\|/2 - na\delta\delta\lambda/4 = 0.171\,\text{m/s} & u_{R2} = u_{R1} + \pi = 2\pi \\ \delta v_{N1} = +na\|\delta\delta\mathbf{i}\|/2 = 0.162\,\text{m/s} & u_{N1} = \text{atan}\left(\delta\delta i_y/\delta\delta i_x\right) = -\pi/2 \\ \delta v_{N2} = -na\|\delta\delta\mathbf{i}\|/2 = -0.162\,\text{m/s} & u_{N2} = u_{N1} + \pi = \pi/2 \end{cases} \quad (18)$$

In the equation above *u* represents the location of the maneuvers along the orbit. For the selected e/i-vectors the radial maneuvers are always located at the ascending and descending nodes (i.e., u = π, 2π), while the cross-track maneuvers are always located at the extreme northern or southern latitudes (i.e., u = ±π/2). This is also shown with the illustration of the transfer below (Figure 4).

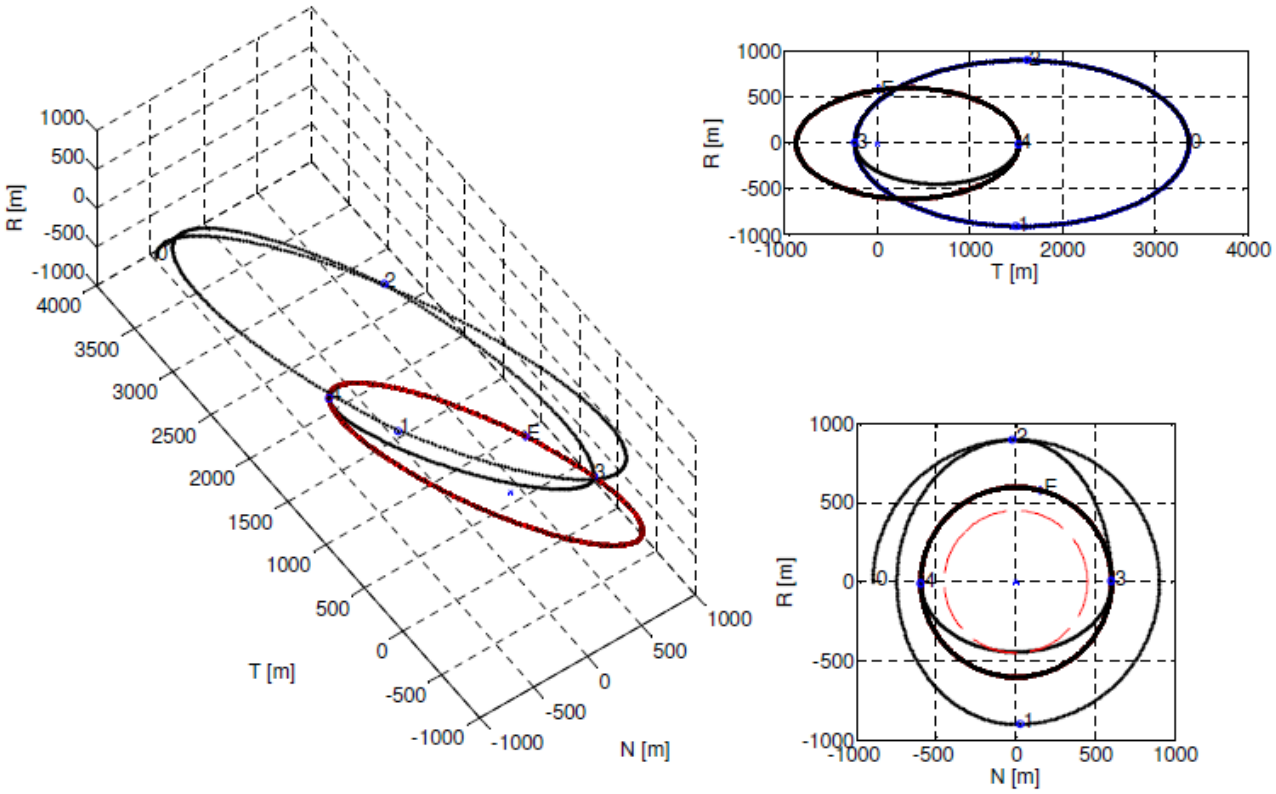

Figure 4. Complete formation reconfiguration using double radial and cross-track impulsive maneuvers from Eq. (16). The resulting relative position is mapped in the RTN orbital frame (black relative trajectories). The labels 1 to 4 indicate the location of the maneuvers. The labels 0 and E indicate the relative position at start and at the rendezvous entry point. The desired final relative orbit and the collision avoidance regions are illustrated in solid and dash red lines.

6.3 Formation Keeping

The relative motion of the two spacecraft is mainly affected by Earth's oblateness perturbations. More specific the relative eccentricity vector follows a circular motion in the e-vector plane, while the relative inclination vector experiences a linear drift proportional to the inclination difference. The latter effect can be removed by selecting a relative ascending node of zero (i.e., ϑ = 0), like selected for the nominal relative orbital elements (Eq. 16).

By defining control windows centered on the nominal values it is possible to keep the formation by exploitation of the aforementioned natural secular motion (Figure 5).

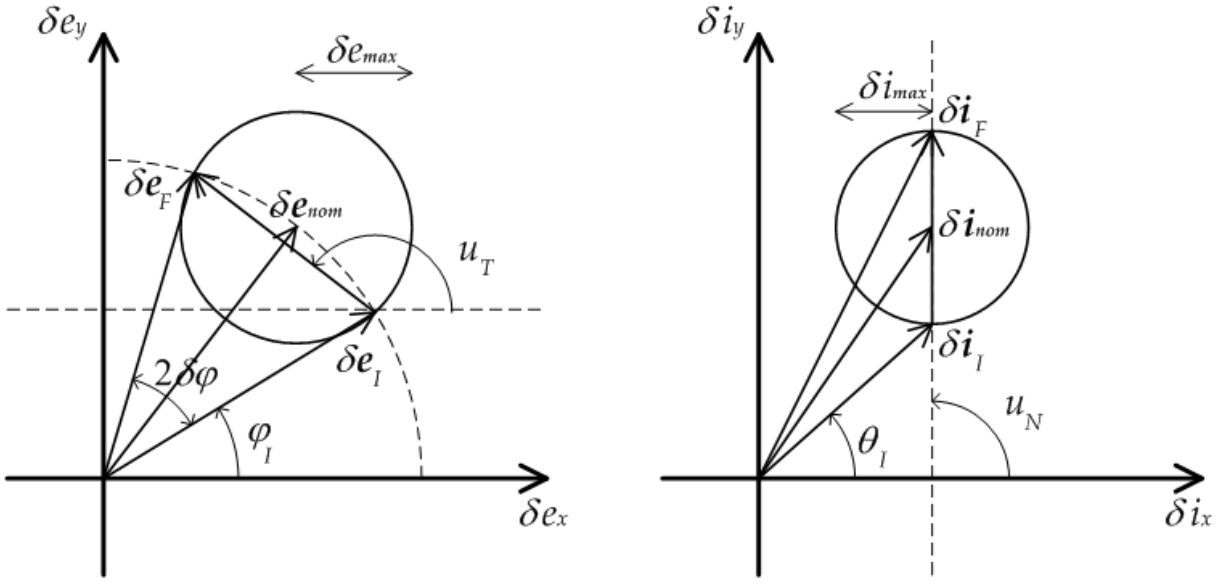

Figure 5. Graphical representation of the control windows for the relative eccentricity vector (left) and the relative inclination vector (right). The subscript *nom* stands for nominal configuration, *max* for maximum allowed deviation from nominal, *I* and *F* for quantities before and after the execution of maneuvers.

The desired relative eccentricity and inclination vectors after performing formation keeping maneuvers are given by

$$\delta\mathbf{e}_F = \begin{Bmatrix} \delta e_{nom_x}\cos(\delta\varphi) - \delta e_{nom_y}\sin(\delta\varphi) \\ \delta e_{nom_x}\sin(\delta\varphi) + \delta e_{nom_y}\cos(\delta\varphi) \end{Bmatrix} \qquad \delta\mathbf{i}_F = \begin{Bmatrix} \delta i_{nom_x} \\ \delta i_{nom_y} - \mathrm{sign}(\delta i_x)\delta i_{\max} \end{Bmatrix}. \tag{19}$$

The subscript nom represents the nominal configuration (Eq. (10)) while $\delta\varphi$ and $\delta i_{\max}$ are maximum tolerated deviations. Eq. (19) can be used to determine the relative e/i-vectors after each orbit control maneuver. As described above the control maneuvers only have to correct the relative e-vector for the developed on-orbit servicing representative scenario. This can be achieved by a pair of along-track maneuvers at the ascending and descending nodes (Eq. (20)). Even though a couple of radial maneuvers could be used as well the fuel efficient version is preferred this time since the maneuvers are small and the separation during formation flight is rather large.

$$\begin{cases} \delta v_{T1} = +na\left\|\delta\delta\mathbf{e}\right\|/4 \approx +na\delta e\sin(\delta\varphi)/2 & u_{T1} = \mathrm{atan}\left(\delta\delta e_y/\delta\delta e_x\right) \approx 0 \\ \delta v_{T2} = -na\left\|\delta\delta\mathbf{e}\right\|/4 \approx -na\delta e\sin(\delta\varphi)/2 & u_{T2} = u_{T1} + \pi \approx \pi \end{cases} \tag{20}$$

For such a strategy the ΔV budget is dependent on the length of the relative eccentricity vector δe and the allowed deviation $\delta\varphi$. For the scenario above with $a\delta e = 900$ m the daily ΔV sums up to

$$\delta v_T = \left|\delta v_{T1}\right| + \left|\delta v_{T2}\right| \approx na\delta e\sin(\delta\varphi) \approx 0.0608\,\mathrm{m/s} \tag{21}$$

7 Conclusion

Within the presented work the absolute navigation accuracy analysis lead to the selection of radar tracking measurements for client and GPS navigation solution data for ground based servicer navigation. Moving forward, the relative navigation analysis resulted in the derivation of a minimum separation safety threshold in the NR-plane, which amounted to 450 m. Thus in the context of former formation flying missions [3][4][5] a nominal formation geometry is designed based on the concept of eccentricity/inclination vector separation. With the implementation of the formation reconfiguration strategy using maneuver couples in radial and cross-track direction an inherently safe capability to transfer to the rendezvous entry point is established. In this context the e/i-vector separation is applied to proximity operations of on-orbit servicing spacecraft for the first time. Future research has to consider relative navigation sensors and the definition of a corresponding approach strategy. Especially the handover between absolute and relative navigation will be of interest. Another field for future work is the derivation of a more elaborate safety threshold by inclusion of differential drag effects in the navigation accuracy analysis. Finally real flight data will be used to evaluate the performance of different relative motion models and their impact on the formation flying design.

8. References

[1] Klinkrad, H., ”Space Debris: Models and Risk Analysis”, Springer-Praxis Books in Astronautical Engineering, Springer-Verlag, 2006.

[2] D'Amico, S., “Autonomous Formation Flying in Low Earth Orbit”, PhD thesis, Technical University of Delft, ISBN 978-90-5335-253-3, 2010.

[3] Montenbruck, O. and Kirschner, M. and D'Amico, S. and Bettadpur, S., “E/I-vector separation for safe switching of the GRACE formation”, Aerospace Science and Technology, Vol. 10, No. 7, pp. 628-635, 2006.

[4] D’Amico, S. and Montenbruck, O., “Proximity operations of Formation-Flying Spacecraft Using an Eccentricity/Inclination Vector Separation”, Journal of Guidance, Control and Dynamics, Vol. 29, No. 3, pp. 554, 2006.

[5] D’Amico, S. and Ardaens, J.S. and De Florio, S., “Autonomous Formation Flying Based on GPS – PRISMA Flight Results”, 6th International Workshop on Satellite Constellation and Formation Flying, Taipei, Taiwan, 1.-3. November, 2010.

[6] Aida, S. and Patzelt, T. and Leushacke, L. and Kirschner, M. and Kiehling, R., “, 21st International Symposium on Space Flight Dynamics, Toulouse, France, 28. Sep. – 2. Oct., 2009.

[7] Brouwer, D., “Solution of the problem of artificial satellite theory without drag”, The Astronomical Journal, Vol. 64, No. 1274, pp. 378–397, 1959.

[8] Lyddane, R.H., “Small eccentricities or inclinations in the Brouwer theory of the artificial satellite”, The Astronomical Journal, Vol. 68, No. 8, pp. 555–558, 1963.

[9] Eckstein, M.C. and Rajasingh, C.K. and Blumer, P., “Colocation strategy and collision avoidance for the geostationary satellites at 19 degrees west”, International Symposium on Space Flight Dynamics, Toulouse, France, 6.-10. November, 1989.

[10] De Florio, S., D’Amico, S., “Collision Risk Assessment for Co-Orbiting Spacecraft”, DEOS-DLR-TN-02, Version 1.0, 28. April, 2010.